# Lecture notes on topological insulators

Ming-Che Chang

*Department of Physics, National Taiwan Normal University, Taipei, Taiwan*

(Dated: January 2, 2025)

## CONTENTS



## I. TOPOLOGICAL INSULATOR

In this Lecture Note, the term "topological insulator" (TI) specifically refers to the insulator with its topology protected solely by time-reversal symmetry. A related term is topological crystalline insulator, in which the topology is protected by crystalline symmetry. We will first study 2D TI, then 3D TI. The edge states of the TIs is the subject of next Lect.

### A. Time-reversal symmetry

For a state with spin quantum number $j$, which can be an integer or a half-integer, the time-reversal operator is

$$\Theta = e^{-iJ_y\pi/\hbar}K, \tag{1.1}$$

in which $J_y$ is a spin operator (Sakurai, 1985). For spin 1/2,

$$\Theta = e^{-is_y\pi/\hbar}K = -i\sigma_y K. \tag{1.2}$$

In general, if a particle has *integer spin*, then applying the TR transformation twice gives $\Theta^2 = 1$. However, if a particle has *half-integer spin*, then

$$\Theta^2 = -1. \tag{1.3}$$

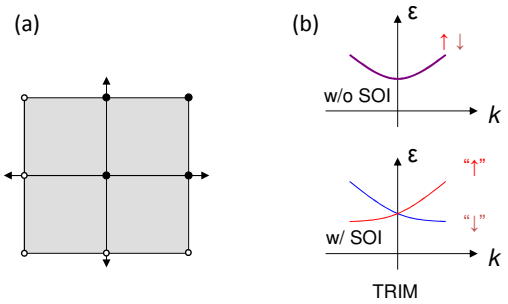


FIG. 1 (a) The TRIM are shown as black and white dots in the first Brillouin zone. Only four of them (black dots) are independent. (b) The Bloch energy levels of a system with time-reversal symmetry but without space-inversion symmetry.

This fact is crucial to the existence of the **Kramer degeneracy**: For a system with TRS and *half-integer* spin, if $\psi$ is an energy eigenstate, then $\Theta\psi$ is also an energy eigenstate. Furthermore, these two states are degenerate and orthogonal to each other.

*Pf*: Since $H\Theta = \Theta H$, so if $\psi$ is an eigenstate with energy $\varepsilon$, $H\psi = \varepsilon\psi$, then

$$H\Theta\psi = \Theta H\psi = \varepsilon\Theta\psi. \tag{1.4}$$

That is, $\Theta\psi$ is also an eigenstate with energy $\varepsilon$. Furthermore, using the identity $\langle\beta|\alpha\rangle = \langle\tilde{\alpha}|\tilde{\beta}\rangle$, one has

$$\langle\psi|\Theta\psi\rangle = \langle\Theta(\Theta\psi)|\Theta\psi\rangle \tag{1.5}$$
$$= -\langle\psi|\Theta\psi\rangle, \tag{1.6}$$

in which $\Theta^2 = -1$ has been used to get the second equation. Therefore, $\langle\psi|\Theta\psi\rangle = 0$. QED.

For example, if a Bloch state $\psi_{n\mathbf{k}\uparrow}$ has energy $\varepsilon_{n\mathbf{k}\uparrow}$, then its time-reversed state $\Theta\psi_{n\mathbf{k}\uparrow} = \psi_{n-\mathbf{k}\downarrow}$ has energy $\varepsilon_{n-\mathbf{k}\downarrow}$, and with time reversal symmetry, $\varepsilon_{n\mathbf{k}\uparrow} = \varepsilon_{n-\mathbf{k}\downarrow}$ (Kramer degeneracy).

#### 1. Time-reversal-invariant momentum

For a solid with space inversion symmetry, one has $\varepsilon_{n-\mathbf{k}s} = \varepsilon_{n\mathbf{k}s}$ ($s = \uparrow$ or $\downarrow$). When the solid has *both* TR and SI symmetries, there is a two-fold degeneracy at each $\mathbf{k}$-point,

$$\varepsilon_{n\mathbf{k}s} = \varepsilon_{n-\mathbf{k}-s} = \varepsilon_{n\mathbf{k}-s}. \tag{1.7}$$

An energy band thus has a *global* two-fold degeneracy over the whole Brillouin zone.

On the other hand, if there is TRS but no SIS, so that $\varepsilon_{n-\mathbf{k}s} \neq \varepsilon_{n\mathbf{k}s}$, then the two-fold degeneracy at a $\mathbf{k}$-point is not guaranteed, except at the $\mathbf{k}$-point that differs from $-\mathbf{k}$ by a **reciprocal lattice vector G**,

$$\mathbf{k} = -\mathbf{k} + \mathbf{G}. \tag{1.8}$$

These $\mathbf{k}$-points are called **time-reversal-invariant momenta** (TRIM), see Fig. 1(a). At a TRIM,

$$\varepsilon_{n\mathbf{k}s} = \varepsilon_{n-\mathbf{k}-s} = \varepsilon_{n,-\mathbf{k}+\mathbf{G},-s} = \varepsilon_{n\mathbf{k}-s}. \tag{1.9}$$

Typical TRIM are located at the corners of a BZ, $\mathbf{k} = \mathbf{G}/2$.

#### 2. Spin-orbit interaction

The spin of an electron in a solid is often coupled with the electron's orbital motion via the **spin-orbit interaction** (SOI),

$$H_{so} = \lambda_{so}\boldsymbol{\sigma} \times \mathbf{p} \cdot \nabla V_L, \ \lambda_{so} = \frac{e\hbar}{4m^2c^2}, \tag{1.10}$$

where $V_L$ is the lattice potential. Such an interaction is invariant under time-reversal symmetry (TRS), and invariant under space-inversion symmetry (SIS) *if* $V_L(-\mathbf{r}) = V_L(\mathbf{r})$. Because of the SOI, Bloch states $\psi_{n\mathbf{k}\pm}$, which are energy eigenstates, are in general not spin eigenstates $\psi_{n\mathbf{k}\uparrow/\downarrow}$.

Recall that the TR operator for fermion is,

$$\Theta = -i\sigma_y K, \ \Theta^2 = -1. \tag{1.11}$$

In the presence of TRS, *if* the Bloch states are topologically trivial, then for one Kramer pair one can choose

$$\begin{cases} \Theta\psi_{n\mathbf{k}+} = -\psi_{n-\mathbf{k}-}, \\ \Theta\psi_{n\mathbf{k}-} = +\psi_{n-\mathbf{k}+}. \end{cases} \tag{1.12}$$

The $-$ sign in front of $\psi_{-\mathbf{k},-}$ is necessary because $\Theta^2 = -1$.

The Bloch states, which are spinors now, are of the form,

$$\psi_{n\mathbf{k}+}(\mathbf{r}) = e^{i\mathbf{k}\cdot\mathbf{r}}\left[+a_{n\mathbf{k}}(\mathbf{r})\chi_\uparrow + b_{n\mathbf{k}}(\mathbf{r})\chi_\downarrow\right], \tag{1.13}$$

$$\psi_{n\mathbf{k}-}(\mathbf{r}) = e^{i\mathbf{k}\cdot\mathbf{r}}\left[-b^*_{n\mathbf{k}}(\mathbf{r})\chi_\uparrow + a^*_{n\mathbf{k}}(\mathbf{r})\chi_\downarrow\right], \tag{1.14}$$

where $a_{n\mathbf{k}}, b_{n\mathbf{k}}$ are cell-periodic functions, and $\chi_\uparrow = (1,0)^T, \chi_\downarrow = (0,1)^T$. If the SOI is weak, then $|b_{n\mathbf{k}}(\mathbf{r})| \ll 1$, so that $(+,-) \simeq (\uparrow,\downarrow)$. It is not uncommon to refer to $\pm$ simply as spin up/down.

For a crystal with time-reversal symmetry, $\varepsilon_{n\mathbf{k}s} = \varepsilon_{n-\mathbf{k}-s}$. In the absence of spin-orbit interaction (SOI), $\varepsilon_{n-\mathbf{k}-s} = \varepsilon_{n-\mathbf{k}s}$ and we have a symmetric energy spectrum with global two-fold degeneracy (Fig. 1(b)). In the presence of SOI, the global two-fold degeneracy is lifted (except at TRIM). Nonetheless, the energy spectrum still looks symmetric because of the Kramer degeneracy.

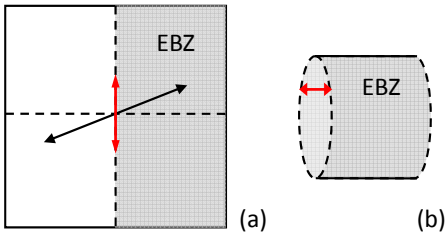


FIG. 2 (a) Time reversal conjugate pairs and effective Brillouin zone. (b) Folding the EBZ into a cylinder, with open edges.

If the Bloch states are topologically non-trivial, then one needs to write

$$\begin{cases} \Theta\psi_{n\mathbf{k}+} = -e^{i\chi_{n-\mathbf{k}}}\psi_{n-\mathbf{k}-}, \\ \Theta\psi_{n\mathbf{k}-} = +e^{i\chi_{n\mathbf{k}}}\psi_{n-\mathbf{k}+}. \end{cases} \tag{1.15}$$

It's possible *not* to have such phase factors (in the so-called **TR-smooth gauge**). However, this would result in points of gauge singularity within the BZ.

### B. $Z_2$ topological number

#### 1. Chern number

To understand the topology in topological insulator (TI), we follow Moore and Balent's argument for 2D TI (Moore and Balents, 2007). Because of time-reversal symmetry, the degenerate Bloch states for $\mathbf{k}$ and $-\mathbf{k}$ in a Brillouin zone are time-reversal conjugate (see Fig. 2(a)). As their Berry curvatures cancel with each other, the first Chern number for a filled band vanishes. Since the domain of *independent* Bloch states cover only half of the BZ (called **effective Brillouin zone**, or EBZ), one may wonder if the integral of the Berry curvature over the EBZ could be quantized.

Unfortunately, since the EBZ does not form a closed surface (see Fig. 2(b)), no quantization is guaranteed. To fix this, one can put two caps with TR conjugation to close the EBZ. This closed surface should have an integer $C_1$, but its value depends on the caps of choice. Nevertheless, because of the TR conjugation, the caps can only change $C_1$ by an even integer. That is, $C_1$ mod 2 is independent of the caps of choice. Therefore, $C_1$ mod 2 should be an intrinsic property of the EBZ itself. We thus have two topological classes: 0 being the usual insulator, and 1 being the topological insulator. Hence, a 2D TI is characterized by a $Z_2$ topological number.

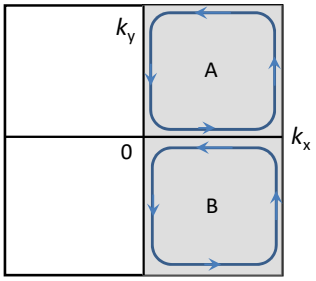


FIG. 3 Two patches of gauge in the EBZ.

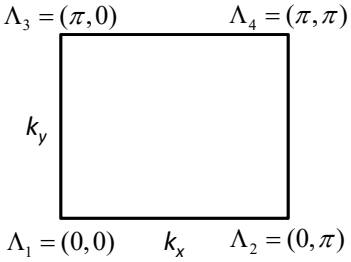


FIG. 4 The first quadrant of the Brillouin zone in a 2D lattice model. The four corners are the TRIM.

### 2. Winding number

Fu and Kane showed that the $Z_2$ topological number can be related to the winding number between two patches of gauge (Fu and Kane, 2006), which we now explain.

First, instead of Eq. (1.15), we will adopt the TR-smooth gauge,

$$\begin{cases} \Theta\psi_{n\mathbf{k}+} = -\psi_{n-\mathbf{k}-}, \\ \Theta\psi_{n\mathbf{k}-} = +\psi_{n-\mathbf{k}+}. \end{cases} \tag{1.16}$$

As a result, the phases of Bloch states cannot be uniquely defined over the whole BZ. As in the case of the magnetic monopole in Chap **??**, we need to use more than one patch of gauge to get rid of singularities. This is the *topological obstruction* mentioned earlier.

Fig. 3 shows the EBZ covered by two patches of gauge. Along their boundary, the cell-periodic functions are connected by gauge transformation,

$$|u_{n\mathbf{k}\alpha}\rangle_B = U_{\alpha\beta}|u_{n\mathbf{k}\beta}\rangle_A, \tag{1.17}$$

where $\alpha, \beta$ are "spin" indices $\pm$, and $\mathsf{U}$ is a U(2) matrix for one Kramer pair.

Recall that the Berry connection and Berry curvature for band $n$ are,

$$\mathbf{A}^n_{\alpha\beta}(\mathbf{k}) = i\langle u_{n\mathbf{k}\alpha}|\frac{\partial}{\partial\mathbf{k}}|u_{n\mathbf{k}\beta}\rangle, \tag{1.18}$$

$$\mathsf{F}^n_{k\ell} = \partial_k \mathsf{A}^n_\ell - \partial_\ell \mathsf{A}^n_k - i[\mathsf{A}^n_k, \mathsf{A}^n_\ell], \tag{1.19}$$

where $k, \ell$ are space indices 1, 2, 3. Under a gauge transformation ($n$ is dropped for simplicity),

$$\mathsf{A}^B_\ell = \mathsf{U}^\dagger \mathsf{A}^A_\ell \mathsf{U} + i\mathsf{U}^\dagger \frac{\partial}{\partial k_\ell}\mathsf{U}. \tag{1.20}$$

The topology of the Bloch states can be characterized by the winding number $w$ of the U(1) phase of $\mathsf{U}$ around the closed loop $\partial A$ in Fig. 3,

$$w = \frac{1}{2\pi i}\oint_{\partial A} d\mathbf{k}\cdot \mathrm{tr}\left(\mathsf{U}^\dagger \frac{\partial}{\partial\mathbf{k}}\mathsf{U}\right). \tag{1.21}$$

Taking the trace of Eq. (1.20), we have

$$w = \frac{1}{2\pi}\oint_{\partial A} d\mathbf{k}\cdot\left(\mathbf{A}^A - \mathbf{A}^B\right), \tag{1.22}$$

in which $\mathbf{A}^{A/B} \equiv \mathrm{tr}\,\vec{\mathsf{A}}^{A/B}$.

Since $|u^A_{\mathbf{k}\alpha}\rangle$ is smoothly defined inside $A$, one has

$$\oint_{\partial A} d\mathbf{k}\cdot\mathbf{A}^A = \int_A d^2k\ F^A_z. \tag{1.23}$$

The same cannot be done for $|u^B_{\mathbf{k}\alpha}\rangle$, since it is *not* smoothly defined in $A$. Instead, we write

$$\begin{aligned}\oint_{\partial A} d\mathbf{k}\cdot\mathbf{A}^B &= \oint_{\partial EBZ} d\mathbf{k}\cdot\mathbf{A}^B - \oint_{\partial B} d\mathbf{k}\cdot\mathbf{A}^B \\ &= \oint_{\partial EBZ} d\mathbf{k}\cdot\mathbf{A}^B - \int_B d^2k\ F^B_z\end{aligned} \tag{1.24}$$

Finally, combine Eqs. (1.23) with (1.24), we have (Fu and Kane, 2006),

$$w = \frac{1}{2\pi}\left(\int_{EBZ} d^2k\ F_z - \oint_{\partial EBZ} d\mathbf{k}\cdot\mathbf{A}\right) \mathrm{mod}\ 2. \tag{1.25}$$

A modulo operation is imposed, since the second term is only gauge invariant modulo 2. This expression of $w$ is different from the Chern number in systems with quantum Hall conductance, which only has the first term, and is an integral over a closed surface (the whole BZ).

Eq. (1.25) looks like the generalized **Gauss-Bonnet formula** for an open 2D surface $M$, in which the Berry curvature is replaced by the *Gaussian curvature* $G$, and the Berry connection is replace by the *geodesic curvature* $k_g$ of the boundary,

$$\chi = \frac{1}{2\pi}\left(\int_M d^2r\ G - \oint_{\partial M} dr\ k_g\right). \tag{1.26}$$

For example, for a torus, $\chi = 0$, for a disk-like surface (which has a boundary), $\chi = 1$, and for a sphere, $\chi = 2$.

### 3. Alternative form of the $Z_2$ topological number

Fu and Kane found yet another way of calculating the $Z_2$ index (Fu and Kane, 2006). Its deduction is less straightforward compared to the ones above, so here we will not explain how it is derived. Detailed explanation can be found in another set of my note.

Let's consider $N$ filled Kramer pairs of Bloch bands in an insulator, and introduce the following quantity,

$$w_{m\alpha,n\beta}(\mathbf{k}) \equiv \langle u_{m-\mathbf{k}\alpha}|\Theta|u_{n\mathbf{k}\beta}\rangle, \quad n=1,\cdots,N; \alpha,\beta=\pm \tag{1.27}$$

They are the matrix elements of a $2N\times 2N$ matrix, often called the **sewing matrix**. Since the Bloch states from different bands are orthogonal to each other, one has

$$w_{m\alpha,n\beta}(\mathbf{k}) = \delta_{mn} w_{n\alpha\beta}(\mathbf{k}). \tag{1.28}$$

For example, for one Kramer pair, the sewing matrix is

$$\mathsf{w}_n = \begin{pmatrix} 0 & e^{i\chi_{n\mathbf{k}}} \\ -e^{i\chi_{n-\mathbf{k}}} & 0 \end{pmatrix}. \tag{1.29}$$

At a TRIM, it becomes an antisymmetric matrix,

$$\mathsf{w}_n = w_n(\mathbf{\Lambda}) \begin{pmatrix} 0 & 1 \\ -1 & 0 \end{pmatrix}, w_n(\mathbf{\Lambda}) \equiv e^{i\chi_{n\Lambda}}. \tag{1.30}$$

For *filled* bands at *each* TRIM, one can define

$$\delta_i = \prod_{n \text{ filled}} \frac{w_n(\Lambda_i)}{\sqrt{w_n^2(\Lambda_i)}}. \tag{1.31}$$

Note that if the argument of a complex number $z = re^{i\theta}$ is restricted to $[0, 2\pi)$, then $\sqrt{z^2}$ has two possible values: If $\theta \in [0,\pi)$, then

$$\frac{z}{\sqrt{z^2}} = \frac{re^{i\theta}}{r\left(e^{2i\theta}\right)^{1/2}} = 1. \tag{1.32}$$

However, if $\theta \in [\pi, 2\pi)$, then

$$\frac{z}{\sqrt{z^2}} = \frac{re^{i(\pi+\tilde{\theta})}}{r\left(e^{2i\tilde{\theta}}\right)^{1/2}}, \ \tilde{\theta}\in[0,\pi] \tag{1.33}$$

$$= -1. \tag{1.34}$$

Thus, $z/\sqrt{z^2}$ can be $+1$ or $-1$. That is, the $\delta_i$ above is product of $+1$ and $-1$.

Finally, the $Z_2$ topological index $\nu$ of a topological insulator is related to $\delta_i$'s (see Fig. 4),

$$(-1)^\nu = \delta_1\delta_2\delta_3\delta_4. \tag{1.35}$$

#### 4. Lattice with inversion symmetry

Even though $\nu$ is known to have two possible values, 0 and 1, it is not easy to get explicit values of $\chi_{n\Lambda_i}$. Fortunately, *if the lattice has space inversion symmetry* (SIS), then we can determine $\nu$ from the parity $\zeta_n(\Lambda_i)$ of the Bloch state $\psi_{n\Lambda_i\pm}$ at TRIM.

If the lattice has SIS, then $\psi_{n\mathbf{k}\alpha}$ are parity eigenstates at $\mathbf{k}=\Lambda_i$,

$$\Pi\psi_{n\Lambda_i\alpha}(\mathbf{r}) = \zeta_{n\Lambda_i}\psi_{n\Lambda_i\alpha}(\mathbf{r}). \tag{1.36}$$

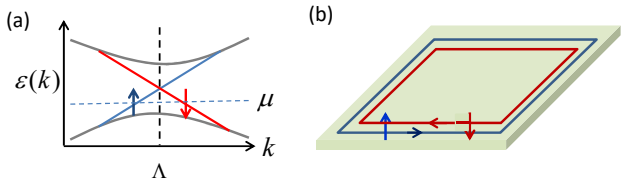


FIG. 5 (a) In momentum space, the energy dispersion curves of the edge states cross each other at a TRIM. (b) In real space, there are helical edge states along the boundary of a 2D TI.

The parity eigenvalue $\zeta_{n\Lambda_i} = 1$ or $-1$ is the same for the two Bloch states (with $\alpha = \pm$) in a Kramer pair. Fu *et al.*, 2007 showed that

$$w_n(\Lambda_i) = \zeta_n(\Lambda_i), \tag{1.37}$$

hence

$$\delta_i = \prod_{n\in\text{filled}} \zeta_n(\Lambda_i). \tag{1.38}$$

It is the cumulative parity of filled Bloch states (pick only one $\zeta_n(\Lambda_i)$ for each Kramer pair) at a TRIM. Finally,

$$(-1)^\nu = \prod_{i=1}^{4} \delta_i. \tag{1.39}$$

Band inversion often results in a change of the parity $\zeta_n$, and this results in topological phase transition. For a crystal without inversion symmetry, one can deform it to one that has SIS and determine its $\nu$ by parities. This is a valid shortcut only *if* the energy gap remains open during the process of deformation.

The 2D topological insulator is often called the **quantum spin Hall** (QSH) insulator. Some proposed materials for QSH insulator are 2D transition metal dichalcogenides (such as the 1T' form of $WTe_2$) (Cazalilla *et al.*, 2014, Qian *et al.*, 2014), and single-layer $ZrTe_5$ (Weng *et al.*, 2014, Li *et al.*, 2016). Several experimental reports can be found in, e.g., Fei *et al.*, 2017, Wu *et al.*, 2018, and Ugeda *et al.*, 2018.

### C. Helical edge state

The energy levels of of edge states appear within the energy gap. According to the discussion at the beginning of this Lect, the energy levels of a TI edge state must cross with its Kramer partner at TRIM. Slightly away from a TRIM, the energy dispersion is linear: one level has positive slope (an edge electron with positive velocity), and the other has negative slope (negative velocity) (see Fig. 5(a)). Note that it's impossible for both to have the same sign of slopes near the degenerate point. This point degeneracy can be lifted *only if* the TRS is broken.

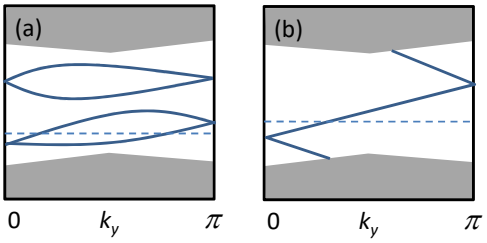


FIG. 6 The energy dispersion of edge states in edge Brillouin zone: (a) trivial 2D insulator, (b) 2D topological insulator.

When the chemical potential is slightly above or below the degenerate point, the Fermi surface would simultaneously cut through a Kramer pair of Bloch states with energies $(\varepsilon_{\mathbf{k}+}, \varepsilon_{-\mathbf{k}-})$. As a result, there is a pair of edge states, with one spin moving along one direction, and the opposite spin moving along the opposite direction (see Fig. 5(b)). This is called **helical edge states**.

In the presence of TRS, the energy levels of edge states would cross each other at TRIM, no matter whether there is topology or not. However, the ways they link together are different. When $\delta_1\delta_2$ and $\delta_3\delta_4$ in Fig. 4 have the same sign, $\nu = 0$, and we have a trivial insulator with no switch of Kramer-pair partner (Fig. 6(a)). When $\delta_1\delta_2$ and $\delta_3\delta_4$ have opposite signs, $\nu = 1$, and we have a TI accompanied by a switch of Kramer-pair partner at TRIM (Fig. 6(b)).

If one plots a horizontal line (chemical potential) inside the energy gap, then it would cut the edge states in $(a)$ even number of times, but cut those in $(b)$ odd number of times. The former can be avoided by shifting or distorting the energy levels of edge states, while the latter cannot be avoided. Thus, the edge states in TI are robust, while those in trivial insulator are not.

The edge state is robust as long as TRS is maintained. Even if there is a non-magnetic impurity $V_{imp}(\mathbf{r})$ blocking the way, the electron will not be back scattered since that requires a spin flip. Indeed, in the *Born approximation*, the transition amplitude for an edge state $\psi_e$ being scattered to its time-reversed state $\theta\psi_e$ is proportional to the square of

$$\langle\psi_e|V_{imp}(\mathbf{r})|\theta\psi_e\rangle. \tag{1.40}$$

Such a bracket can be shown to be zero.

If there is a *magnetic impurity* that breaks TRS, then an electron could be backscattered, accompanied by a spin flip. Also, in the presence of *electron interaction*, there is a possibility that the edge is spontaneously magnetized. Should this happen, then the edge state is no longer protected by the TRS.

**Exercise**

1. Under a gauge transformation,

$$\begin{pmatrix} u'_{\mathbf{k}+} \\ u'_{\mathbf{k}-} \end{pmatrix} = \mathsf{U} \begin{pmatrix} u_{\mathbf{k}+} \\ u_{\mathbf{k}-} \end{pmatrix}, \tag{1.41}$$

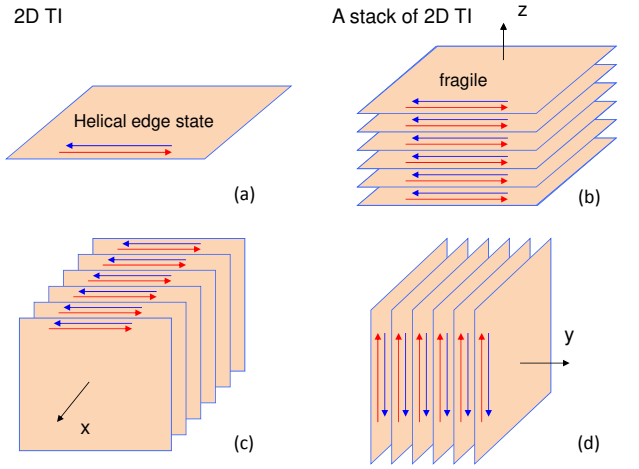


FIG. 7 (a) A 2D TI and its helical edge state. (b) Stacking 2D TIs to construct a 3D TI. The surface state is not as robust as the edge state of a 2D TI. (c) and (d): Stacking the 2D TIs along the other two directions. The helical edge states reside on different sides of the 3D cubes.

and

$$\mathbf{A}' = \mathbf{A} + i\mathrm{tr}\left(\mathsf{U}^\dagger \frac{\partial}{\partial \mathbf{k}} \mathsf{U}\right). \tag{1.42}$$

It is known that a unitary matrix can diagonalized as

$$\mathsf{U} = \mathsf{S}^\dagger \mathsf{D} \mathsf{S}, \tag{1.43}$$

with

$$\mathsf{D} = e^{i\alpha} \begin{pmatrix} e^{i\theta} & 0 \\ 0 & e^{-i\theta} \end{pmatrix}. \tag{1.44}$$

With these, show that under a gauge transformation, the line integral in Eq. (1.25) could change by an even integer.
2. Prove that the transition amplitude for an edge state $\psi_e$ being scattered to its time-reversed state $\theta\psi_e$ is zero,

$$\langle\psi_e|V_{imp}(\mathbf{r})|\theta\psi_e\rangle = 0. \tag{1.45}$$

## II. 3D TOPOLOGICAL INSULATOR

The analysis of the 2D TI can be generalized to 3D. One can naively stack the 2D materials to form a 3D structure (see Fig. 7). In early days, this has been attempted to build a 3D quantum Hall system, but failed. An essential reason is that there is no Chen number in odd dimension. The situation is different for the case of TI, where one can actually build a *weak* TI this way.

To simplify the discussion, consider a cubical BZ (see Fig. 8). If the insulator has TRS, then $\mathbf{k}$-state and $-\mathbf{k}$-state are TR conjugate. In particular, the points on the $xy$ plane map to themselves under time reversal. According to the Moore-Balents argument, this plane should

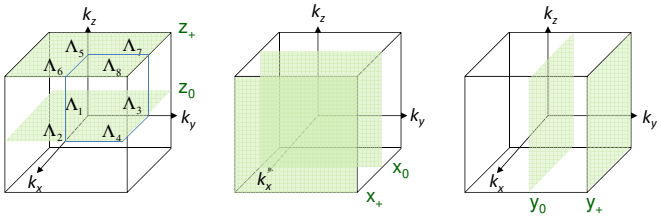


FIG. 8 The colored 2D planes in the 3D BZ are time reversal invariant. That is, under a TR transformation, they are mapped to themselves. There are all six of them. Each plane can be assigned a $Z_2$ topological number.

have a corresponding $Z_2$ index. Using Fu and Kane's formula, it is given by

$$(-1)^{\nu} = \delta_1\delta_2\delta_3\delta_4 \equiv z_0, \tag{2.1}$$

where $\delta_i = \prod_{n\in \text{ filled}} \zeta_n(\Lambda_i)$ (see Fig. 8).

By symmetry, the $k_y$-$k_z$ plane and the $k_z$-$k_x$ plane also have their own $Z_2$ indices, $x_0$ and $y_0$. In addition, the planes at front, right, and top side of the cube also map to themselves under time reversal. So there are three more $Z_2$ indices, $x_+$, $y_+$, and $z_+$. Overall there are 6 $Z_2$ numbers.

However, these numbers are not independent of each other,

$$x_0x_+ = y_0y_+ = z_0z_+ = \prod_{i=1}^{8}\delta_i. \tag{2.2}$$

Because of these two relations, there are only 4 independent $Z_2$ integers. One can choose, for example,

$$(z_0z_+, x_+, y_+, z_+) \quad \text{or} \quad (\nu_0;\nu_1,\nu_2,\nu_3), \tag{2.3}$$

where

$$(-1)^{\nu_0} = \prod_{i=1}^{8}\delta_i, \tag{2.4}$$

$$(-1)^{\nu_1} = \delta_2\delta_4\delta_6\delta_8, \tag{2.5}$$

$$(-1)^{\nu_2} = \delta_3\delta_4\delta_7\delta_8 \tag{2.6}$$

$$(-1)^{\nu_3} = \delta_5\delta_6\delta_7\delta_8. \tag{2.7}$$

Among these 4 indices, $\nu_0$ is called **strong TI index**; $\nu_1,\nu_2,\nu_3$ are called **weak TI indices**. The strong index is intrinsic to the 3D TI, while the other 3 are, roughly speaking, related to the stacking of 2D TIs along the $x$, $y$, and $z$ directions (see Fig. 7). These indices are discovered by Moore and Balents, 2007, Fu *et al.*, 2007, and Roy, 2009 at about the same time.

### A. Fermi circle of the surface state

In Fig. 9(a), four examples of the cumulative parity distributions at TRIM are shown. The product of all 8 parities gives $(-1)^{\nu_0}$. The product of four cumulative parities on the $k_y$-$k_z$ plane at $k_x = \pi$ gives $(-1)^{\nu_1}$, and so on. This way, one can get the four indices $(\nu_0;\nu_1,\nu_2,\nu_3)$ shown on top of the figures.

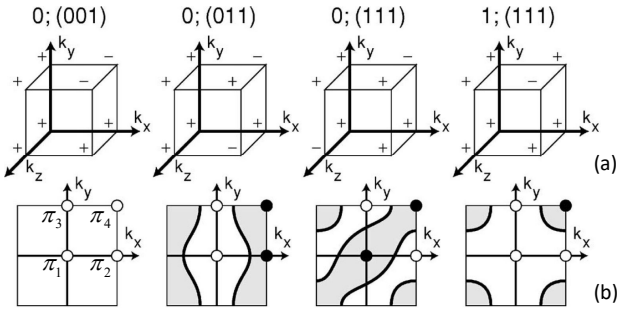


FIG. 9 (a) Four examples of the parity distributions at the TRIM (in the first octant of the BZ) of 3D TIs. (b) The Fermi seas in surface BZs of the four cases in (c). White and black dots at the corners show the product of parities along $k_z$ (see text). The grey areas are filled, and the white areas are empty. (Figs from Fu and Kane, 2007)

Recall that for a 2D TI, the energy level of an edge state within the energy gap would inevitably cross with the chemical potential (Fig. 6 of Lect I). This applies to 2D planar subspaces of the 3D Brillouin zone. For example, suppose the TI has an open surface on the $x-y$ plane. Fig. 9(b) shows the 2D surface BZ of the surface state (SS) on the $k_x$-$k_y$ plane. The parities $\pi_i$ on corners are the products of two parities along the $k_z$-direction. When $\pi_1\pi_2 = -1$ (e.g., see the 2nd figure from the left in Fig. 9(b)). There is one (or an odd number of) edge state traversing the energy gap from $k_x = 0$ to $\pi$, crossing the chemical potential $\mu$ at a Fermi point. On the other hand, since $\pi_1\pi_3 = 1$, there is no (or an even number of) edge state crossing $\mu$. The Fermi point at $k_y = 0$ becomes a Fermi line when one scans over $k_y$.

That is, once we know the four parities $\pi_i$, the topology of the Fermi circle in the 2D surface BZ can be determined (assuming the energy dispersion of a SS crosses the Fermi level only once): between a black dot (odd parity) and a white dot (even parity), there must be a Fermi line separating filled states from empty states. One can check that the Fermi circles in Fig. 9(b) do follow this rule. The Fermi sea encloses one or more black dots, which are also the locations of Dirac points (in 2D momentum space).

Fig. 10 sums up nicely what we have learned so far. When the compound BiTlSe undergoes a phase transition from an ordinary insulator to a strong TI, the band inversion, the change of parity at TRIM, and the helical surface states with spin-momentum locking all emerge simultaneously.

In general, a strong TI would have odd number of Dirac points, and odd pairs of helical SS. On the other hand, a weak TI always have even number of Dirac points, and even pairs of helical SS. The Dirac point of a weak TI is

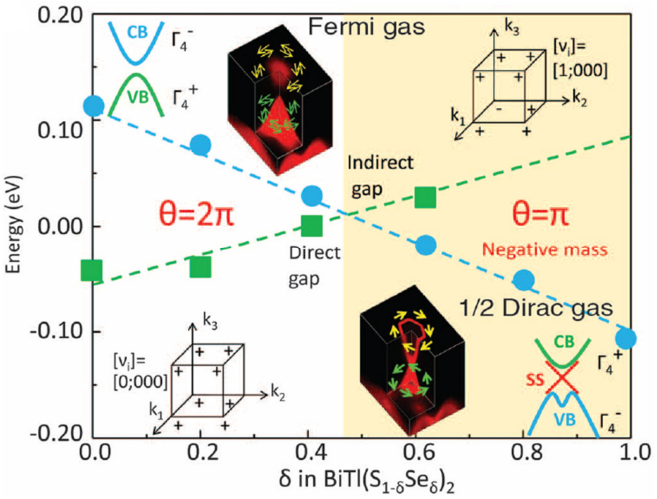


FIG. 10 Phase transition of topological insulator and accompanied changes. BiTlSe is a trivial insulator when $\delta < 0.47$. All of the parities at the corners are positive, and each Bloch state can have two spins. There is a band inversion when $\delta = 0.47$, causing the parity at the origin to change sign. As a result, the material becomes a topological insulator. It now has helical edge states, in which the direction of spin is locked with the direction of momentum (see the ARPES data in dark insets). Fig from Xu *et al.*, 2011

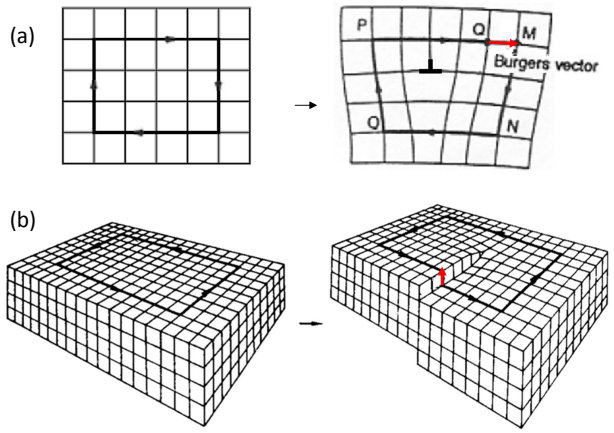


FIG. 11 (a) For a lattice with an edge dislocation, the Burgers vector is perpendicular to the line of dislocation. (b) For a lattice with screw dislocation, the Burgers vector is parallel to the line of dislocation.

fragile. Take the one with indices $(0; 011)$ as an example: Suppose that due to *surface reconstruction*, a unit cell is doubled along the $y$-direction. As a result, the surface BZ would be folded back along the $k_y$-direction. The two black dots now could couple with each other and open the Dirac point.

Note that even though for a strong TI, there are odd number of Dirac points on *one* surface, there are more Dirac points on the opposite side of the TI. When counted together, a 3D TI would still have even number of Dirac points from its surface states.

BiSb is the first experimentally confirmed 3D topological insulator (Hsieh *et al.*, 2008). Subsequently, many more have been predicted and verified (Bansil *et al.*, 2016). An ideal TI would be one that is an *insulator* with *large band gap*. But this is hard to come by, because the inversion of energy gap is often a result of spin-orbit coupling, which is not easy to be enhanced. More comments on topological materials can be found in Sec. II.D below.

### B. Weak topological indices

As we have mentioned earlier, a weak TI with indices $(0; 0, 0, 1)$ can be considered as layers of 2D TIs stacked along the $z$-axis. For general weak indices, one can define

$$\mathbf{M}_\nu = \nu_1 \frac{\mathbf{g}_1}{2} + \nu_2 \frac{\mathbf{g}_2}{2} + \nu_3 \frac{\mathbf{g}_3}{2}, \tag{2.8}$$

in which $\mathbf{g}_i$ are basis of reciprocal lattice vectors, then the 2D-TI layers are stacked along the $\mathbf{M}_\nu$ direction.

Even though a weak 3D TI has fragile 2D surface states, it can have robust 1D states along a line of dislocation. In Fig. 11(a), one can see that due to a line of dislocation along $\mathbf{t}$, a loop that is closed in a perfect crystal now can no longer be closed. The vector of displacement $\mathbf{B}$ is called a **Burgers vector**. For an **edge dislocation**, $\mathbf{B} \perp \mathbf{t}$; for a **screw dislocation**, $\mathbf{B} \parallel \mathbf{t}$.

It is shown by Ran *et al.*, 2009 that, if

$$\mathbf{B} \cdot \mathbf{M}_\nu = \pi \pmod{2\pi}, \tag{2.9}$$

then there is a pair of helical edge states along the line of dislocation (Fig. 12). For example, consider a cubic lattice with indices $(0; 0, 0, 1)$, then $\mathbf{M}_\nu = \mathbf{g}_3/2 = \pi/a\hat{z}$, where $a$ is the lattice constant. If there is a screw dislocation with $\mathbf{B} = a\hat{z}$ (see Fig. 11(b)), then $\mathbf{B} \cdot \mathbf{M}_\nu = \pi$, and there are 1D helical states along the line of dislocation. If $\mathbf{B} = a\hat{x}$ or $a\hat{y}$ (for edge dislocation), then there is no edge state in this weak TI.

This criterion applies to both strong and weak TIs. For example, if $\nu_0 = 1$, but $\mathbf{M}_\nu = 0$, then none of the dislocation lines would have helical edge states.

### C. Bulk-edge correspondence

Surface (or edge) state has been a recurring theme in this course. At the interface between two materials with different topological electronic phases, the interface states are bound to exist. This is called the **bulk-edge correspondence**. So far, we have discussed the domain-wall state in SSH model, the chiral edge state in quantum Hall system, and the helical edge states in 2D and 3D TIs. We will see more examples of surface state later, when new topological phases are encountered.

Even though a general proof is lacking, such a bulk-edge correspondence is generally believed to be true (for

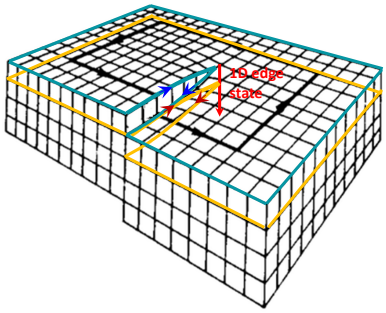


FIG. 12 In a 3D weak TI with screw dislocation, each plane can be considered as a 2D insulator with a cut ending at the line of dislocation. Near the cut, the opposing edge channels from adjacent planes cancel with each other. As a result, the edge electrons would move down the line of dislocation.

*non-interacting* systems). This property can roughly be understood as follows: In the sense of Thomas-Fermi approximation, energy gap can be defined locally and vary with location. Near the interface between two different topological phases, the energy gap needs to close (e.g., for band inversion), otherwise the topological phase could not change. As a result, there must be a gapless region near the interface (or surface) for electrons to dwell on.

A remark: For a quantum topological phase to change, the energy gap needs be closed. Such a statement is valid only if the symmetry of the system remains unchanged. *If* the symmetry changes, then can pass from one phase to the other *without* closing the gap (Ezawa *et al.*, 2013). For example, consider the SSH model,

$$H = (t_- + t_+ \cos k)\sigma_x + t_+ \sin k\ \sigma_y + m\sigma_z, \qquad (2.10)$$

where $t_\pm = t \pm \delta$, $\delta$ is the dimerization parameter (see Prob. 2 of Chap **??**). The energy spectrum is

$$E_\pm = \pm\sqrt{t^2 \cos^2 \frac{k}{2} + \delta^2 \sin^2 \frac{k}{2} + m^2}. \qquad (2.11)$$

When $m = 0$, $H$ has both TRS and particle-hole symmetry. To get from the phase with $\delta > 0$ to the one with $\delta < 0$, we need to cross the gapless point $(\delta, m) = (0, 0)$, see Fig. 13. However, if $m \neq 0$, then $H$ has no TRS and the energy bands are gapped. In this case, one can go from a phase with $\delta > 0$ ($m = 0$) to a phase with $\delta < 0$ ($m = 0$) via a path with non-zero $m$, such that the energy gap remains open during the transit.

### D. Topological crystalline insulator and beyond

In addition to TRS, the topology of an insulator can also be protected by crystalline symmetry. These are called **topological crystalline insulator** (TCI). As we have learned, $T^2 = -1$ plays a crucial role in TI. In a TCI, this is not required and $T^2 = 1$ is allowed. That is,

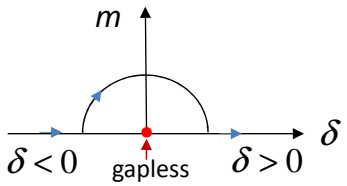


FIG. 13 In the parameter space of $(\delta, m)$, the SSH model is gapless only at a single point $(0, 0)$.

electron spin, as well as spin-orbit coupling, is no longer essential to the topology.

The surface states need to cross each other at $\mathbf{k}_i$, similar to the SS in a topological insulator. However, some other aspects of the SS are different. For example, their energy dispersion near the crossing point is quadratic in Fu's example, instead of linear. Also, the number of Dirac points on a surface can be even, instead of odd. Note that even though the gapless Dirac point is protected by the $UT$ symmetry, the rotation symmetry could be damaged by structural deformation.

In some other TCIs, the TR symmetry can be dispensed with, so that only the crystalline symmetry is at play. The first experimentally confirmed TCI is SnTe (Hsieh *et al.*, 2012), which is protected by a mirror symmetry.

This discovery opens up a floodgate to topological materials, since there are hundreds of crystalline symmetry groups. With the help of the so-called *symmetry-based indicators* (Po *et al.*, 2017) or *elementary band representations* (Bradlyn *et al.*, 2017), researchers can search through the database of materials to find out candidates of topological materials. See Gibney, 2018, Tang *et al.*, 2019, Queiroz and Stern, 2020, and Elcoro *et al.*, 2021 for some updates.

A related development is the discovery of **higher-order TCIs**. They have conducting SS protected by topology along edges (2nd order), or corners (3rd order) of the topological material. Also, see Parameswaran and Wan, 2017 and the references therein.

The topology in TI and TCI are protected by time-reversal symmetry and crystalline symmetry. They belong to a larger class of topological phases called **symmetry-protected topological (SPT) phases**. The famous **Haldane phase** of odd-integer spin chain is another example of the SPT phase. It is protected by SO(3) spin symmetry. In addition, there are also topological phases *not* related to (and protected by) symmetry, such as the **fractional quantum Hall state**.

## REFERENCES

Bansil, A, Hsin Lin, and Tanmoy Das (2016), "Colloquium: Topological band theory," Rev. Mod. Phys. **88**, 021004.

Bradlyn, Barry, L. Elcoro, Jennifer Cano, M. G. Vergniory, Zhijun Wang, C. Felser, M. I. Aroyo, and B. Andrei

Bernevig (2017), "Topological quantum chemistry," Nature **547**, 298 EP –.

Cazalilla, M A, H. Ochoa, and F. Guinea (2014), "Quantum spin hall effect in two-dimensional crystals of transition-metal dichalcogenides," Phys. Rev. Lett. **113**, 077201.

Elcoro, Luis, Benjamin J. Wieder, Zhida Song, Yuanfeng Xu, Barry Bradlyn, and B. Andrei Bernevig (2021), "Magnetic topological quantum chemistry," Nature Communications **12** (1), 5965.

Ezawa, Motohiko, Yukio Tanaka, and Naoto Nagaosa (2013), "Topological phase transition without gap closing," Scientific Reports **3**, 2790 EP –.

Fei, Zaiyao, Tauno Palomaki, Sanfeng Wu, Wenjin Zhao, Xinghan Cai, Bosong Sun, Paul Nguyen, Joseph Finney, Xiaodong Xu, and David H. Cobden (2017), "Edge conduction in monolayer wte2," Nature Physics **13**, 677–682.

Fu, Liang, and C. L. Kane (2006), "Time reversal polarization and a $Z_2$ adiabatic spin pump," Phys. Rev. B **74**, 195312.

Fu, Liang, and C. L. Kane (2007), "Topological insulators with inversion symmetry," Phys. Rev. B **76**, 045302.

Fu, Liang, C. L. Kane, and E. J. Mele (2007), "Topological insulators in three dimensions," Phys. Rev. Lett. **98**, 106803.

Gibney, Elizabeth (2018), "Trove of exotic matter thrills physicists," Nature **560**, 151.

Hsieh, D, D. Qian, L. Wray, Y. Xia, Y. S. Hor, R. J. Cava, and M. Z. Hasan (2008), "A topological dirac insulator in a quantum spin hall phase," Nature **452** (7190), 970–974.

Hsieh, Timothy H, Hsin Lin, Junwei Liu, Wenhui Duan, Arun Bansil, and Liang Fu (2012), "Topological crystalline insulators in the snte material class," Nature Communications **3**, 982.

Li, Xiang-Bing, Wen-Kai Huang, Yang-Yang Lv, Kai-Wen Zhang, Chao-Long Yang, Bin-Bin Zhang, Y. B. Chen, Shu-Hua Yao, Jian Zhou, Ming-Hui Lu, Li Sheng, Shao-Chun Li, Jin-Feng Jia, Qi-Kun Xue, Yan-Feng Chen, and Ding-Yu Xing (2016), "Experimental observation of topological edge states at the surface step edge of the topological insulator zrte$_5$," Phys. Rev. Lett. **116**, 176803.

Moore, J E, and L. Balents (2007), "Topological invariants of time-reversal-invariant band structures," Phys. Rev. B **75**, 121306.

Parameswaran, SA, and Y Wan (2017), "Viewpoint: Topological insulators turn a corner," Physics **10**, 1–3.

Po, Hoi Chun, Ashvin Vishwanath, and Haruki Watanabe (2017), "Symmetry-based indicators of band topology in the 230 space groups," Nature Communications **8** (1), 50.

Qian, Xiaofeng, Junwei Liu, Liang Fu, and Ju Li (2014), "Quantum spin hall effect in two-dimensional transition metal dichalcogenides," Science **346** (6215), 1344–1347.

Queiroz, Raquel, and Ady Stern (2020), "Symmetry indicators for topological superconductors," Journal Club for Condensed Matter Physics: www.condmatjclub.org/?p=4161.

Ran, Y, Y Zhang, and A Vishwanath (2009), "One-dimensional topologically protected modes in topological insulators with lattice dislocations," Nat. Phys. **5**, 298.

Roy, Rahul (2009), "Topological phases and the quantum spin hall effect in three dimensions," Phys. Rev. B **79**, 195322.

Sakurai, J J (1985), *Modern quantum mechanics* (Benjamin-Cummings Publishing Company).

Tang, Feng, Hoi Chun Po, Ashvin Vishwanath, and Xiangang Wan (2019), "Efficient topological materials discovery using symmetry indicators," Nature Physics **15** (5), 470–476.

Ugeda, Miguel M, Artem Pulkin, Shujie Tang, Hyejin Ryu, Quansheng Wu, Yi Zhang, Dillon Wong, Zahra Pedramrazi, Ana Martín-Recio, Yi Chen, Feng Wang, Zhi-Xun Shen, Sung-Kwan Mo, Oleg V. Yazyev, and Michael F. Crommie (2018), "Observation of topologically protected states at crystalline phase boundaries in single-layer wse2," Nature Communications **9**, 3401.

Weng, Hongming, Xi Dai, and Zhong Fang (2014), "Transition-metal pentatelluride $ZrTe_5$ and $HfTe_5$: A paradigm for large-gap quantum spin hall insulators," Phys. Rev. X **4**, 011002.

Wu, Sanfeng, Valla Fatemi, Quinn D. Gibson, Kenji Watanabe, Takashi Taniguchi, Robert J. Cava, and Pablo Jarillo-Herrero (2018), "Observation of the quantum spin hall effect up to 100 kelvin in a monolayer crystal," Science **359** (6371), 76–79.

Xu, Su-Yang, Y. Xia, L. A. Wray, S. Jia, F. Meier, J. H. Dil, J. Osterwalder, B. Slomski, A. Bansil, H. Lin, R. J. Cava, and M. Z. Hasan (2011), "Topological phase transition and texture inversion in a tunable topological insulator," Science **332** (6029), 560–564.